Direct Identification of Two Regimes of Metal Particle Combustion using Condense-luminescence

Quan Tran
Texas Tech University
Michelle L. Pantoya (michelle.pantoya@ttu.edu)
Texas Tech University
Igor Altman
Naval Air Warfare Center Weapons Division

Research Article

Keywords: Bomb Calorimeter, Heat of Combustion, Radiant Heat Transfer, Solid Fuels, Powders, Metals, Reactive Materials

Posted Date: March 16th, 2021

DOI: https://doi.org/10.21203/rs.3.rs-289403/v1

Abstract

Experiments were designed to investigate two regimes of metal particle combustion: fast and slow burning regimes. Stress-altering aluminum particles had been shown to produce a distinctly faster burning rate compared to untreated aluminum particles. The root cause for the differences in burning rate had been unclear. In this study, stress-altered and untreated aluminum particles were reacted as dispersed powder in a closed bomb calorimeter designed to monitor the transient temperature changes resulting from energy release upon combustion. The product residue was analyzed for size and species concentration. Results showed metastable γ-alumina that is associated with nano-oxide formation was in substantially higher concentration for stress-altered particle reactions that produced greater energy transfer rates. The increased energy transfer rate corresponded to higher radiant energy emission owing to condensation of nano-oxide particles. This study justifies condense-luminescence as a means for increasing the energy release rate of aluminum particles. By strategically altering metal fuels to control a formation of nano-oxide particles upon combustion, appreciable increases in the radiant energy flux can transform energy release rates.

I. Introduction

High energy density makes metal particles attractive for various applications ranging from ordnance [1], to electronics [2], to pharmaceuticals [3]. For energetic applications, metal powders are typically mixed into a formulation as dispersed powder and provide a fuel source to aid energy generation upon reaction [4]. Despite decades of studies, the mechanism of metal particle combustion is still not well understood and merits further investigation. One major distinction between metal powder combustion and more well-understood hydrocarbon combustion is the formation of metal oxides in the final combustion product. Unlike the gaseous products of hydrocarbon combustion, such as water and carbon dioxide, when metals burn in the vapor–phase regime, condensed nano-oxides are finally formed. Unlike water vapor and carbon dioxide gas, metal nano-oxides condense into liquid or solid phase, which effectively emit radiant energy [5]. The role of radiant emission on energy release rate is often overlooked [6], More recently, the contribution of radiant emission has been recognized as very important in modeling energy exchange processes but the complexities of modeling radiant emission from metal nano-oxides is also widely acknowledged [7].

Besides the significance for quantitative metal combustion modeling, the light emission from combustion-generated nano-oxides is of general scientific importance and constitutes a phenomenon we call “condense-luminescence”. In condense-luminescence, the energy released during condensation of gaseous metal nano-oxides is emitted. In chemiluminescence, chemical heat released leads to excitation of a molecule that is further emitted and chemiluminescence could been used as a diagnostic in studying combustion [8]. The principal difference in condense-luminescence is that condensation leads to excitation of a nanoparticle as a whole, which is why the phenomenon deserves a separate name. Previous work[9] [10] demonstrated that the processes accompanying nano-oxide formation play an essential role in light emission and provide the main energy transport mode for condensation energy

removal. Also, there is huge scatter in nano-alumina emissivities [11] inferred from light emission measurements in flames and based on the equilibrium nature (Planck's law) of radiation. The large scatter in emissivity justifies examination of non-equilibrium nano-oxide light emission [12]. This departure of non-equilibrium should be taken into account when interpreting pyrometry measurements in reactive systems [13].

A comprehensive study investigating the relationship between nano-oxide occurrence and related radiant emission during metal combustion may shed light on a lot of puzzles unresolved to date. In particular, understanding the link between nano-oxide formation and energy release may explain the coexistence of two regimes for aluminum particle combustion recently reported [14]. Altman et al. [14] showed the coexistence of fast and slow combustion regimes for Al particle oxidation that has extremely important implications to energetic applications. They showed that the different temporal character of heat transfer corresponds to different combustion regimes (i.e., a fast and slow regime), but the underlying cause of the temporal differences remains elusive.

The identification of two combustion regimes was realized by pre-stressing aluminum particles using an established annealing and quenching protocol, and their combustion was compared to untreated aluminum particle combustion. In their experiment, single aluminum particles were laser ignited and burn times were measured. The heat pre-treatment of the aluminum particles favored faster burn times whereas untreated Al particles burned in the slower combustion regime [15]. Further investigation into the mechanism responsible for distinctly different temporal heat release regimes could enable engineering strategies that can be used to tailor metal particle combustion for specific energetic applications. Understanding of the nature of these combustion regimes and potential to control them may allow for eliminating the fluorination processing step[16] that is currently being used in order to enhance the performance of metal combustion.

The objective of this study is to directly demonstrate a relationship between the combustion regime and the temporal behavior of heat released during aluminum powder combustion. The experiments are performed within a closed calorimetry bomb under an elevated pressure corresponding to propellant burning conditions. Experiments are performed in pure oxygen gas to ensure complete combustion of the aluminum powder. The calorimeter promotes metal oxidation when aluminum powder is properly dispersed[17] and allows one for confirming complete combustion. Therefore, the degree of combustion completeness is not a variable affecting the temporal heat release measurements. The experimental design also provides transient thermal data to resolve distinctions in the rate of heat released. An X-ray diffraction (XRD) analysis of the products formed enables identification of nano-oxides. The coupled transient thermal response data from the calorimeter and nano-oxide species formation data from XRD analysis are used to distinguish a shift between metal particle combustion regimes.

Ii. Experimental

A. Materials

The aluminum (Al) powders are supplied by Valimet, Inc. with three characteristic Al particle diameters of 3.5 μm, 8 μm, and 108 μm (Valimet Product No. H2, H5, H95, respectively) [18]. The Al powder is shown using Scanning Electron Microscopy (SEM) images in Fig. 1**(a) - (f).** The porous medium used to suspend the powder in the bomb calorimeter is a starch-based packing peanut (PP) composed of poly-carbohydrates (The Office Depot Product # 578 – 376), including corn and potato starches. The PP microstructure has high porosity that provides a readily combustible medium to disperse the powder [17]. For simplicity, as-received powders are referred to as untreated and identified as UN (e.g., UN-H2, UN-H5, and UN-H95) and stress-altered powders using annealing and super-quenching (SQ) pre-treatments described below are identified as SQ (SQ-H2, SQ-H5, and SQ-H95). Figure 1 shows no physical difference in the appearance of SQ and UN particles.

B. Aluminum Stress-Altered

The stress-altered aluminum was annealed and quenched using a custom-built chamber designed to withstand high thermal gradients associated with rapid quenching[19] and shown in Fig. 2. Powder was placed into the chamber and sealed with a high temperature O-ring (-114 S70 SQ, O-ring, Inc.). A K-type thermocouple (BARE-20-K-12, Omega) was inserted on top of the chamber to measure the transient temperature of the powder during annealing and quenching. The chamber was heated from room temperature to 320°C at a rate of 10°C/min using a Neytech Vulcan furnace (Dentsply Cermco). The powders stabilized at 320°C for 10 minutes and quenched in the sealed chamber using a liquid solution composed of 78.6 wt. % water, 9.4 wt. % NaCl, 4.1 wt. % Dawn™ dish soap, and 7.9 wt. % Simple Green™. The quenching rate was an average 900°C/min and relatively fast for powder quenching, such that the aluminum particle heat treatment had previously been called “super-quenched” or SQ Al [19].

C. Calorimetry

Bomb calorimeter experiments were performed for the intrinsic measurement of heat of combustion (ΔH_c). Also, temperature data was extracted throughout the combustion process to examine rates of energy transfer inferred from changes in transient temperature. A Parr 6400 Automatic Isoperibol Calorimeter (Parr Instrument Co.) was used for the experiments. A new technique was recently introduced to accurately measure the energy released during combustion of metal powders. The technique used a porous medium that effectively suspended the powders during combustion to prevent pooling and sintering that can affect combustion. Molten metal pooling inhibits oxidation and alters diffusion reaction processes that otherwise occur for single particles. The dispersing medium was shown to produce aluminum heat of combustion (ΔH_c) measurements on the order of theoretical predictions [17]. The details of the experimental setup are described by Tran et al.[17] but will be summarized here. All powders were used in the range of 0.0375-0.05 g but the porous medium was held constant at 0.10 g. The powder was dispersed in the porous medium and the combined sample placed in a BN crucible inside an 1138 Oxygen Combustion Vessel (Parr Instrument). The ΔH_c was determined by combusting the sample with excess oxygen at a pressure of 30 atm and subtracting the energy content of the dispersing media.

Post burn residue was analyzed using a Rigaku MiniFlex II powder diffractometer. X-ray diffraction (XRD) patterns were obtained by scanning a 2θ range of 5–70°, step size = 0.02°, and scan time of 2 degrees/minute. The X-ray source was Cu Kα radiation (λ = 1.5418 Å) with an anode voltage of 30 kV and a current of 15 mA. Diffraction intensities were recorded on a position sensitive detector (D/teX Ultra).

Iii. Results

A. SEM Analysis

Representative SEM images of the products collected after Al combustion are shown in **Figure 3.** The appearance of both nano- and micro-sized particles aligns with the current understanding of vapor-phase combustion of a metal particle [5] [6]. Specifically, alumina nanoparticles form in the envelope surrounding the burning particle and microparticles result from the formation of an oxide residue that is an essential condition to sustain combustion [20]. Metastable alumina phases are associated with nanoparticle growth because nanoparticle formation involves rapid particle cooling that inherently induces structural defects [21] that result in formation of the metastable phase, i.e., γ-alumina. On the contrary, formation of the micron sized residue, which occurs via surface oxidation of a burning particle and/or deposition of gaseous oxide on the surface, does not involve rapid cooling and thus leads to formation of the stable phase, α-alumina.

B. XRD Analysis

The overlapped XRD patterns of products recovered from UN-H2 and SQ-H2 combustion are shown in **Figure 4**. Graphics for each Al studied are additionally included in *Supplementary Information*, **Fig. S1**. The peaks are indexed as α-alumina and γ-alumina. The stable α-alumina phase corresponds with microparticles while the metastable γ-alumina phase corresponds with nanoparticles. The inset in **Fig. 4** highlights more clearly the relative increased peak intensity for α-alumina in UN-H2 (blue curve) and relative increased peak intensity for γ-alumina in SQ-H2 (red curve).

To qualitatively estimate the relative alumina phase composition, the ratio of areas at the 43.8º peak (α-alumina) and the 46.3º peak (γ-alumina) shown in the inset of **Fig. 4** is analyzed and detailed in *Supplementary Information*. The results are summarized in **Table 1** to quantify the differences in alumina phases associated with each set of experiments. Additionally, **Tables S1-S3** provide similar results for slightly different XRD analysis parameters in *Supplementary Information*. In all tabulated results, combustion of SQ powders consistently produced a larger amount of metastable γ-Al_2O_3 and a smaller amount of stable α- Al_2O_3 compared to combustion of the UN powders. The same trend is also observed for all Al particle sizes.

Table 1. Relative mass fraction of alumina phases in combustion products recovered after aluminum oxidation in the bomb calorimeter.

	UN-H2	SQ-H2	UN-H5	SQ-H5	UN-H95	SQ-H95
α-alumina, %	29	15	14	10	23	13
γ-alumina, %	71	85	86	90	77	87

C. Combustion Experiments

Heat of combustion was measured in the bomb calorimeter. Twenty runs were performed for each of the six types of aluminum powders tested (i.e., UN-H2, UN-H5, UN-H95, SQ-H2, SQ-H5, SQ-H95). Results are summarized in **Table 2**.

Table 2. Results for ΔH_c (kJ/g). The average values of twenty runs and the standard deviations are presented, all data are provided in *Supplementary Information*, Table S4.

UN-H2	SQ-H2	UN-H5	SQ-H5	UN-H95	SQ-H95
29.02±1.19	29.95±0.97	30.45±0.66	30.48±0.80	30.47±0.60	30.74±0.72

The measured ΔH_c is not appreciably different for untreated compared with stress altered powders, as expected for complete combustion. Within the measurement error of less than 5%, all ΔH_c are close to the theoretical ΔH_c of aluminum oxidation, 31.05 kJ/g [22] and confirm complete combustion. The goal of stress-altering particles is to shift the combustion regime from slow to faster time scales. The overall oxidation reaction should produce complete combustion resulting in similar measured heats of combustion. However, the rate of energy release will be different and can be inferred from the transient temperature measurements of heat transfer within the calorimeter.

The transient behavior of the normalized water bath temperature recorded in the calorimeter experiments is a useful parameter for characterizing material combustion [17]. The normalized temperature, ΔT_N, is defined in Eq. (1) and characterizes the instrument's response to the heat released from combustion.

$$\Delta T_N(t) = \frac{T(t) - T_{min}}{T_{max} - T_{min}}, \qquad (1)$$

In Eq. (1), $T(t)$ is recorded time-dependent temperature and T_{max} and T_{min} are maximum and minimum temperatures of the water bath during the combustion experiment.

In **Figure 5a**, the normalized temperatures are shown for all UN powders. The difference between three powders is small and difficult to distinguish because the three curves nearly overlap. To better resolve the differences in normalized transient temperature, **Fig. 5b** shows the ratio of the normalized temperatures for UN-H2 and UN-H5 powders with respect to time. This ratio is noticeably greater than unity at early times representative of the onset of the instrument's response to combustion.

Figure 6 shows the ratio of the normalized temperatures for the SQ and UN powders. When SQ is compared to UN, all three particle sizes exhibit a ratio greater than unity at early times. Note that the non-monotonous behavior of that ratio at later times originates from the complex heat transfer processes associated with the experiment, i.e., heat transfer from the gas to chamber walls within the bomb, heat transfer through the walls, and heat transfer from the walls to the water bath. All these processes have different time scales and the intensity of each process depends on the condition of the experiment. Here we are interested in the onset of the temperature response, which results from the fastest phenomenon.

Table 3 summarizes the normalized temperatures at the onset of the instrument's response to combustion expressed as a percent relative to UN-H2.

Table 3. The normalized temperature of the water bath at the onset of the instrument's response to combustion and the difference between the onset responses for SQ and UN. Data is expressed relative to UN-H2.

	UN-H2	SQ-H2	UN-H5	SQ-H5	UN-H95	SQ-H95
Onset Temperature, %	100	107	107	120	98	106
Onset Temperature Difference, %	7		13		8	

Comparing data in **Table 1 and 3**, there is a direct correlation between the fraction of γ-alumina (i.e., nano-oxide) in the combustion products and the temperature response at the onset of the instrument response to combustion. The larger fraction of γ -alumina in the combustion products corresponds to a higher onset instrument response. More explicitly, generation of metastable γ -alumina associated with nano-oxides leads to a greater energy release rate observed in the calorimeter as a higher normalized temperature at early times.

Iv. Discussion

The correlation between the instrument onset response and the fraction of generated γ -alumina nano-oxides, as well as a noticeable increase in both values for SQ compared to UN powders is the major finding of the current work. In order to understand its significance, a discussion about the peculiarities of heat release during metal combustion and their effect on the closed bomb calorimetry measurements and on the temporal behavior of the water bath temperature follows.

The calorimetry measurements indicate energy transferred by combustion through the bomb walls to the water bath over a time scale of hundreds of seconds. The character of the recorded temporal dependence of the water bath depends on initial temperature conditions driving heat transfer from the bomb wall to the water. Therefore, the initial wall temperature is important. In the case of hydrocarbon combustion, products are gaseous, and energy released from a reaction is dissipated within the gas inside the bomb calorimeter. In this case, the initial wall temperature is not affected. For metal combustion, products are condensed particles, and strong radiant emission by those particles accompanies the heat exchange

process. Being absorbed by the bomb wall, radiant energy exchange leads to an elevated wall temperature just after metal combustion has concluded and leads to a higher onset instrument response temperature. This qualitative analysis of the heat exchange process provides a foundation for our further conclusions and a schematic illustrating the process is shown in Fig. 7.

A major contribution to radiant emission during metal combustion is related to the formation of nano-oxides as a result of the reaction. Light emission is an essential component of the overall energy released during the condensation growth of the nano-oxides [10]. A substantial portion of radiant energy comes from the condensation energy and cannot be described using the equilibrium oxide emissivity. In the case of Al combustion, huge scatter in emissivity is reported for alumina inferred from flame pyrometry measurements [11]. The huge scatter originates from an invalid assumption about the equilibrium character of nano-alumina in the flame. Then, the light emission from nano-oxide formation via condensation is a reaction-induced luminescence, which probably deserves a separate name such as “condense-luminescence”. Based on the above concept, a higher fraction of nano-oxides in the combustion products corresponds to stronger light emission and more radiant energy during combustion, as illustrated in Fig. 7. The latter leads to a higher initial wall temperature, and higher onset instrument response temperature as seen in Fig. 6. Thus, the origin of the experimentally observed relationship between the fraction of γ-alumina (i.e., nano-oxides) and the normalized temperature from the onset instrument response becomes clear: higher normalized temperatures (Fig. 6) are a result of greater radiant energy inherent from the condensation process associated with nano-oxides identified as metastable γ-alumina (Table 1).

The noticeable increase in the fraction of γ-alumina in the combustion products of SQ particles compared to UN in Table 1 means that the corresponding aluminum oxide products form differently. The distinct differences may be a consequence of aluminum particle combustion in two different regimes depending on whether or not particles are stress-altered. Since the presence of micrometer sized alumina in combustion products is an outcome of vapor-phase Al combustion, the change in the mass fraction of α-alumina could be interpreted as a measure of the combustion regime change. Then, based on the data in Table 1 that shows a significant reduction in the mass fraction of α-alumina for SQ particles, the change in the combustion regime is evident. Note that the coexistence of two different combustion regimes for metal particles was discussed in [14]. The coexistence of two combustion regimes depends on the heat transfer at the interface between the particle surface and gas. The intensity of this heat transfer may be controlled by the particle pre-treatment. Thus, the current paper directly demonstrates the regime change is a function of stress-altering the Al particles.

Performing experiments in the closed calorimetry bomb helped confirm the completeness of combustion [17] that was needed for the interpretation of results in this study. However, using the onset of the instrument response to distinguish the nuanced changes in radiant emitted energy is not the best way to characterize fast reaction processes because the differences are small and hard to distinguish, albeit highly repeatable. At the same time, taking into account the large inertia of the water bath (i.e., its long time-scale response), the ability to distinguish the onset instrument response, and therefore the light

emission accompanying the differences in short time-scale metal combustion, means there is a substantial difference in the overall emitted energy between SQ and UN Al experiments.

V. Conclusions

Bomb calorimetry experiments were performed for aluminum powders of varying sizes that were stress-altered and also untreated. Twenty experiments were performed for each of six aluminum powders (i.e., three variations in particle size and two conditions: stress altered and untreated). Further material characterization studies using SEM and XRD were also performed to analyze the size and identify species composition of the powders. Results support previous observations of two distinct regimes of combustion: i.e., fast and slow burning regimes. The SQ Al powders exhibit a higher concentration of nano-oxides evident as metastable γ-alumina phase that correspond to faster rate of energy transfer. The mechanism for that increased rate of energy exchange is explained as an increased contribution of radiant energy emission owing to condensation of nano-oxides. The measurable increase in energy release rate is an indication that condense-luminescence plays a significant role in the overall energy balance associated with metal fuel combustion. Results from this study suggest that strategies to manipulate metal particles to form nano-oxides during reaction may lead to significant gains in radiant energy transfer that result in faster overall energy release rates.

Declarations

AUTHOR'S CONTRIBUTIONS

All authors contributed equally to this work.

COMPETING INTERESTS

All authors declare no competing interests.

DATA AVAILABLITY

The datasets generated during and/or analyzed during the current study are available from the corresponding authors on reasonable request.

ACKNOWLEDGEMENTS

The authors from TTU (MP, QT) are grateful for support from United States Office of Naval Research (ONR) grant number N00014-19-2082 and Dr. Chad Stoltz. Also, I.A. is thankful for funding from the NAVAIR ILIR program managed at the ONR and administered by Dr. Alan Van Nevel. We are grateful to Dr.

Daniel Unruh from the Chemistry Department at TTU for XRD measurement assistance and Mr. Charles (Luke) Croessmann for his support in SEM imaging.

References

[1] E. Price and R. Sigman, "Combustion of Solid Propellants," in Solid Propellant Chemistry, Combustion, and Motor Ballistics, New York, NY: American Institute of Aeronautics and Astronautics, 2000, pp. 663-687.

[2] C. Rossi, K. Zhang, D. Esteve, P. Alphonse, P. Tailhades and C. Vahlas, "Nanoenergetic materials for MEMS: A Review," Journal of Microelectromechanical Systems, vol. 16, no. 4, pp. 919-932, 2007.

[3] K. Stank and H. Steckel, "Physico-Chemical Characterization of Surface Modified Particles for Inhalation," Int. J. of Pharmaceutics, vol. 448, pp. 9-18, 2013.

[4] D. Sundaram, V. Yang and R. Yetter, "Metal-based nanoenergetic materials: synthesis, properties, and applications," Progress in Energy and Combustion Science, vol. 61, pp. 293-365, 2017.

[5] T. Brzustowski and I. Glassman, "Spectroscopic investigation of metal combustion," in Heterogeneous Combustion, H. Wolfhard, I. Glassman and L. Green, Eds., New York, NY: Academic Press, 1964, pp. 41-74.

[6] K. Brooks and M. Beckstead, "Dynamics of Aluminum Combustion," Journal of Propulsion and Power, vol. 11, no. 4, p. 769, 1995.

[7] M. Beckstead, Y. Liang and K. Pudduppakkam, "Numerical simulation of single aluminum particle combustion (Review)," Combustion, Explosion and Shock Waves, vol. 41, pp. 622-638, 2005.

[8] M. Bedard, T. Fuller, S. Sardeshmukh and W. Anderson, "Chemiluminescence as a diagnostic in studying combustion instability in a practical combustor," Combustion and Flame, vol. 213, pp. 211-225, 2020.

[9] Y. Shoshin and I. Altman, "Integral radiation energy loss during single Mg particle combustion," Combustion Science and Technology, vol. 174, no. 8, pp. 209-219, 2002.

[10] I. Altman, P. Pikhitsa and M. Choi, "Key effects in nanoparticle formation by combustion techniques," in Gas Phase Nanoparticle Synthesis, C. Granqvis and L. Kish, Eds., Dordrecht, Kluwer, 2004, pp. 43-67.

[11] V. Bityukov and V. Petrov, "Absorption coefficient of molten aluminum oxide in semitransparent spectral range," Combustion and Flame, vol. 5, pp. 51-71, 2013.

[12] S. De Iuliis, R. Donde and I. Altman, "On pyrometry in particulate-generating flames," Combustion Science and Technology, 2020.

[13] H. Wang, D. Kline and M. Zachariah, "In-operando high-speed microscopy and thermometry of reaction propagation and sintering in a nanocomposite," Nature Communications, vol. 10, p. 3032, 2019.

[14] I. Altman, A. Demko, K. Hill and M. Pantoya, "On the possible coexistence of two different regimes of metal particle combustion," Combustion and Flame, vol. 221, pp. 416-419, 2020.

[15] K. Hill, M. Pantoya, E. Washburn and J. Kalman, "Single particle combustion of pre-stressed aluminum," Materials, vol. 12, p. 1737, 2019.

[16] H. Wang, H. Ren, T. Yan, Y. Li and W. Zhao, "A latent highly activity energetic fuel: thermal stability and interfacial reaction kinetics of selected fluoropolymer encapsulated sub-micron sized Al particles," Scientific Reports, vol. 11, p. 738, 2021.

[17] Q. Tran, P. Dube, M. Malkoun, I. Altman, R. Koch and M. Pantoya, "Bomb calorimeter advancements for evaluating powder metal fuels," Review of Scientific Instruments, 2021.

[18] I. Valimet, "Aluminum H-Series Data Sheet," Valimet, 2017. [Online]. Available: http://valimet.com/wp-contents/uploads/2017/08/Aluminum-H-Series-Data-Sheet-.pdf. [Accessed 01 12 2021].

[19] K. Hill, N. Tamura, V. Levitas and M. Pantoya, "Impact Ignition and Combustion of Micron-Scale Aluminum Particles Pre-Stressed with Different Quenching Rates," Journal of Applied Physics, p. 115903, 2018.

[20] I. Altman and Y. Vovchuk, "Thermal regime of the vapor-state combustion of magnesium particle," Combustion Explosion Shock Waves, vol. 36, pp. 227-229, 2000.

[21] S. De Iuliis, R. Donde and I. Altman, "On thermal regime of nanoparticles in synthesis flame," Chemical Physics Letters, vol. 769, p. 138424, 2021.

[22] S. Fischer and M. Grubelich, "Theoretical energy release of thermites, intermetallic, and combustible metals," Sandia National Laboratory Technical Report SAND98-1176C, Alburguerque, 1998.

Figures

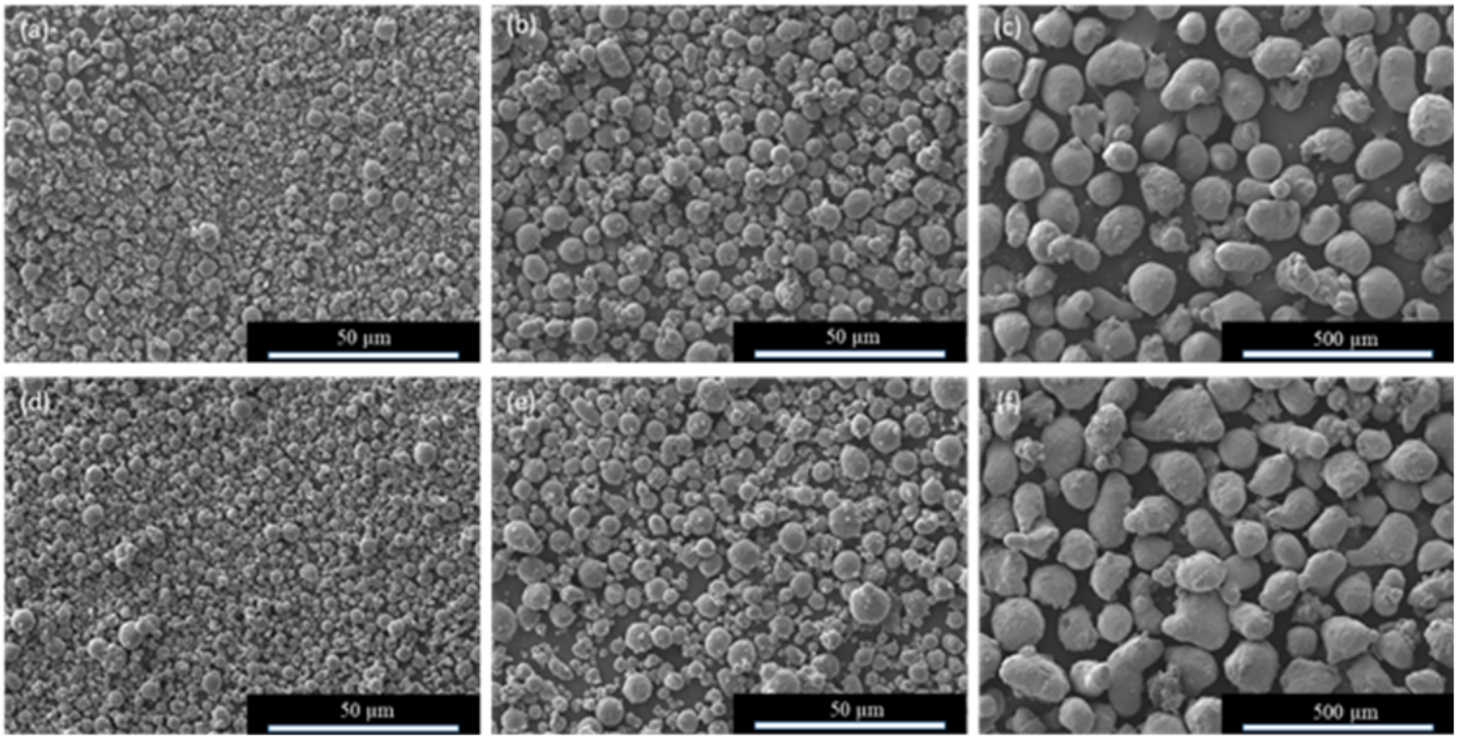

Figure 1

Micrographs from SEM imaging of (a) UN-H2, (b) UN-H5, (c) UN-H95 and (d) SQ-H2, (e) SQ-H5, and (f) SQ-H95. A Hitachi S-4300 SEM was used for imaging and the powder was mounted on carbon adhesive tabs and sputter coated with Palladium.

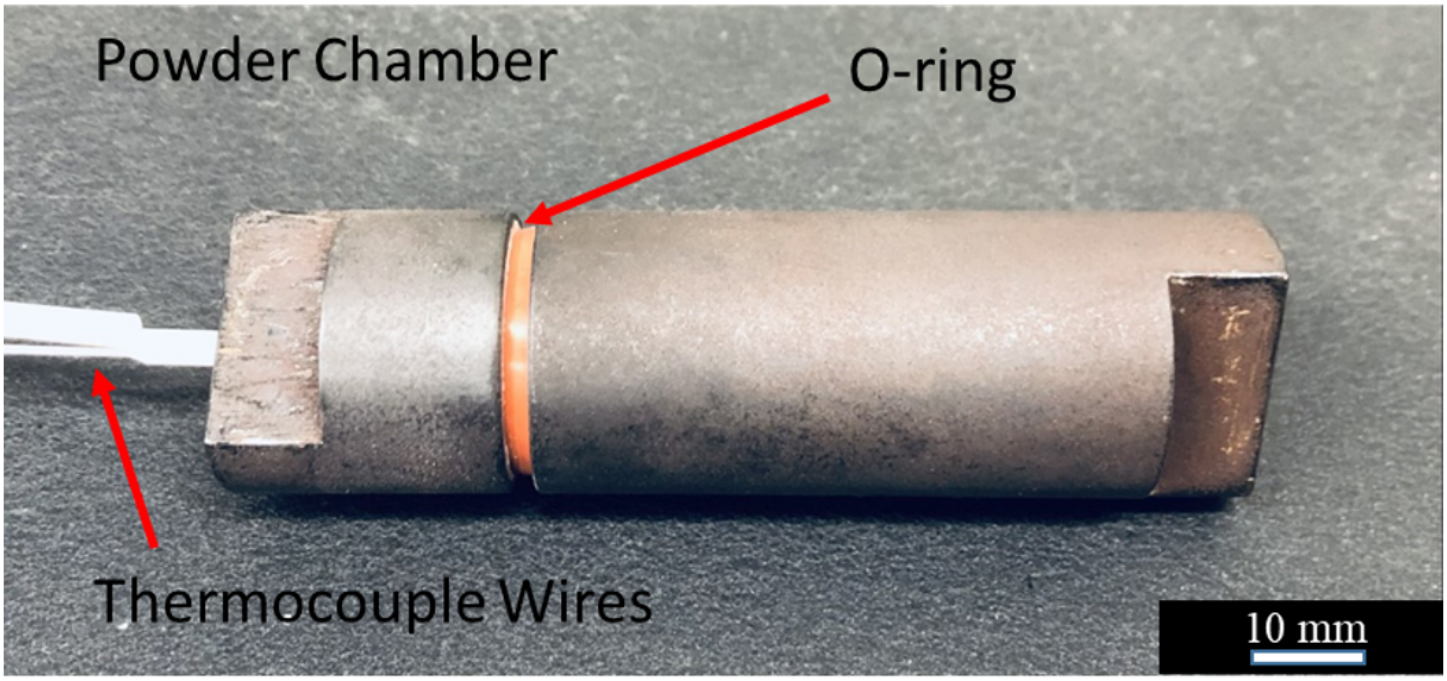

Figure 2

Powder chamber with O-ring seal and thermocouple wires.

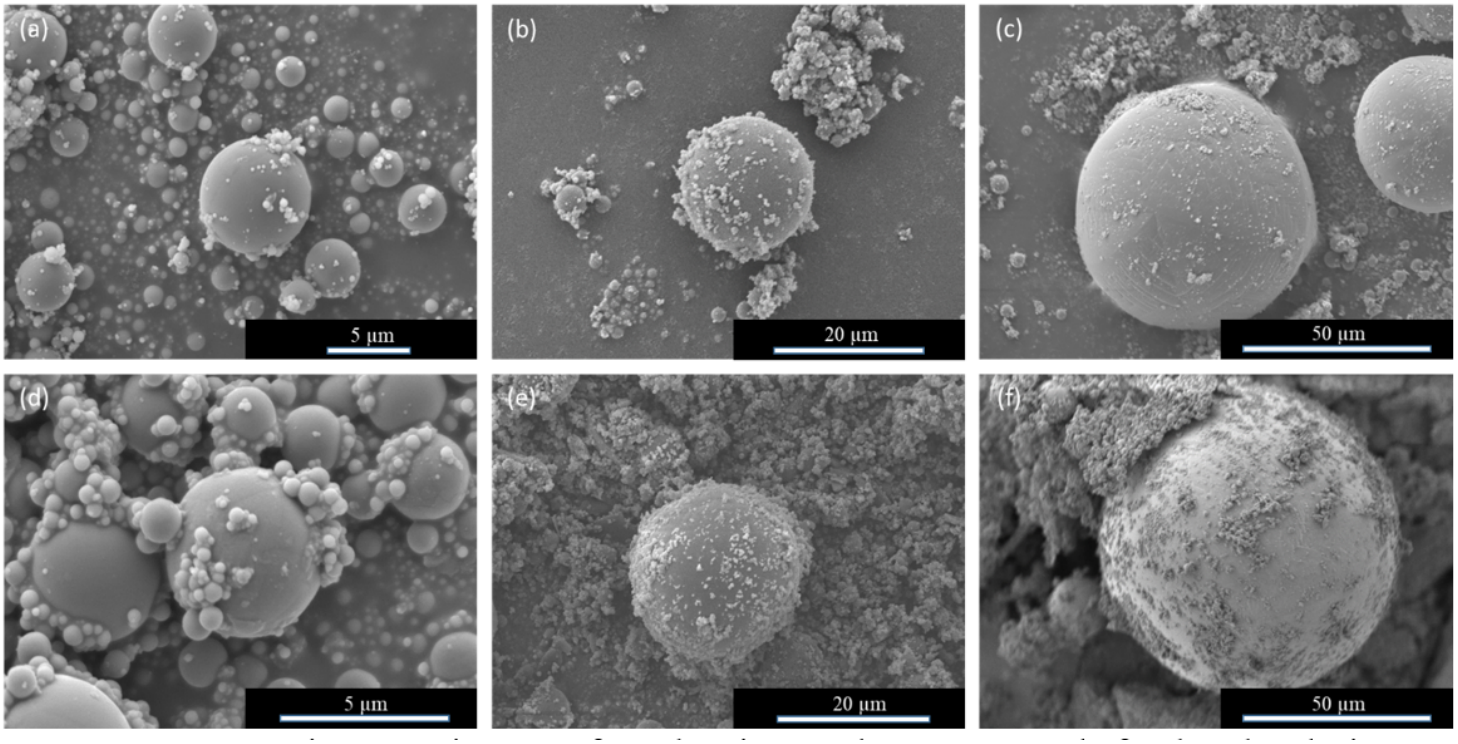

Figure 3

Representative SEM images of combustion products recovered after bomb calorimetry experiments of (a) UN-H2, (b) UN-H5, (c) UN-H95 and (d) SQ-H2, (e) SQ-H5, and (f) SQ-H95. Nanoparticles and microparticles are seen in all recovered residue.

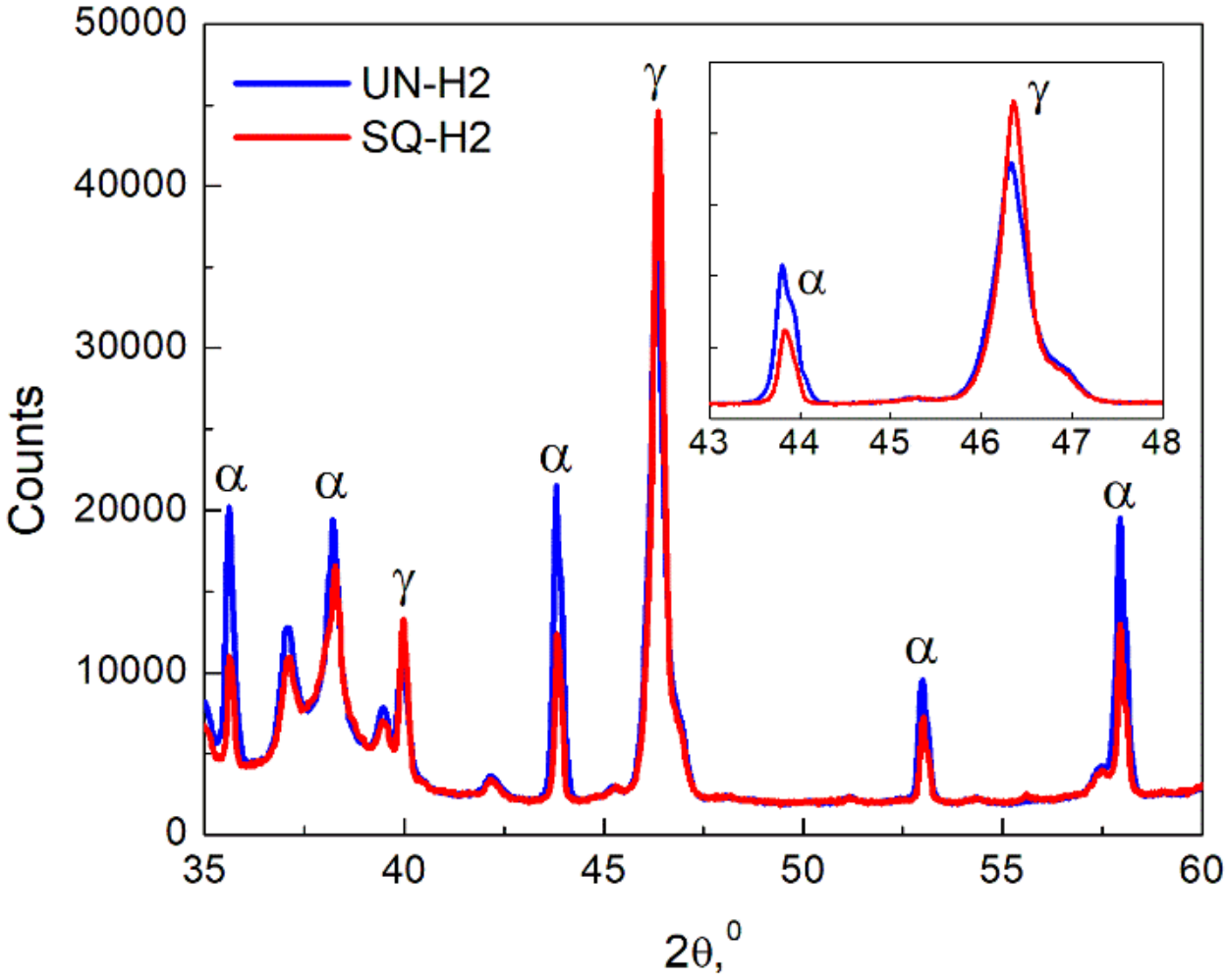

Figure 4

Overlapped XRD patterns of combustion products of UN-H2 and SQ-H2. The insert shows the region of major peaks to highlight the phase composition difference. Additional graphs for H5 and H95 are provided in Supplementary Information.

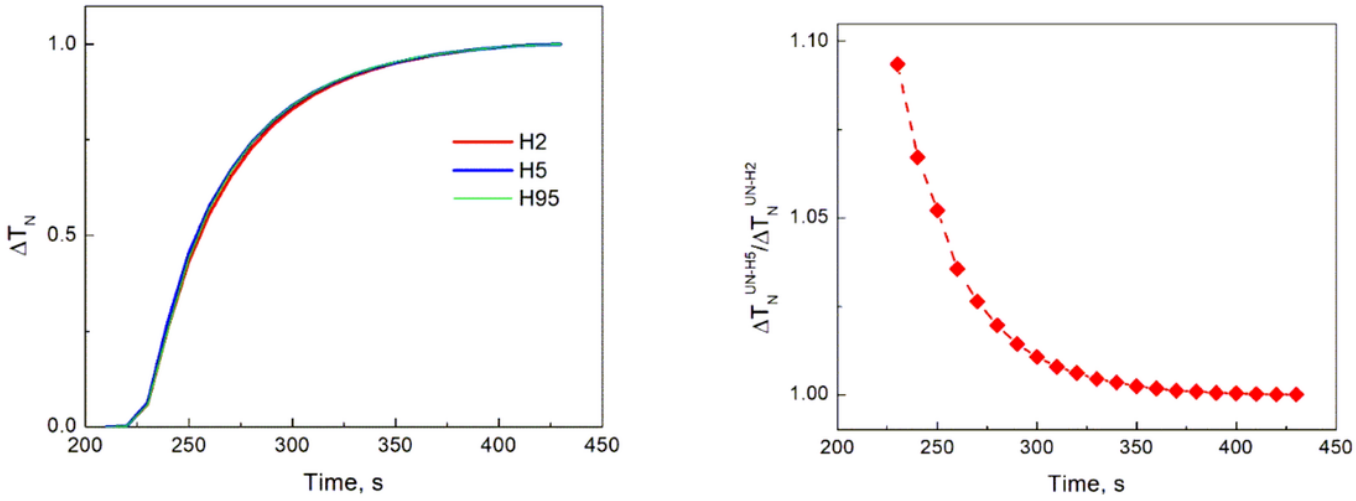

Figure 5

a) The normalized temperature of the water bath in the experiments with the UN powders. b) The ratio of normalized temperatures of the water bath in experiments with two UN powders.

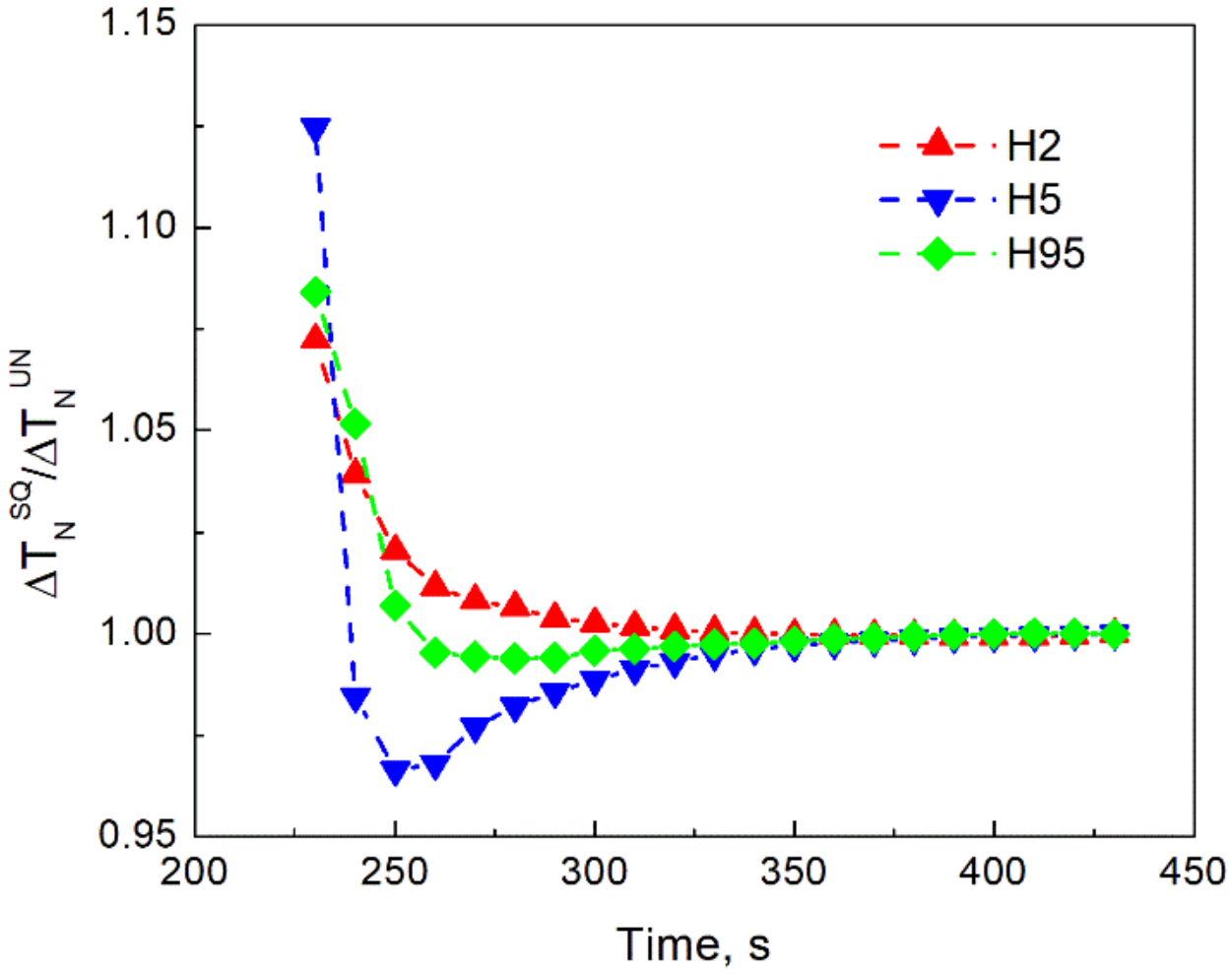

Figure 6

The ratio of normalized temperatures of the water bath in experiments with SQ and UN powders.

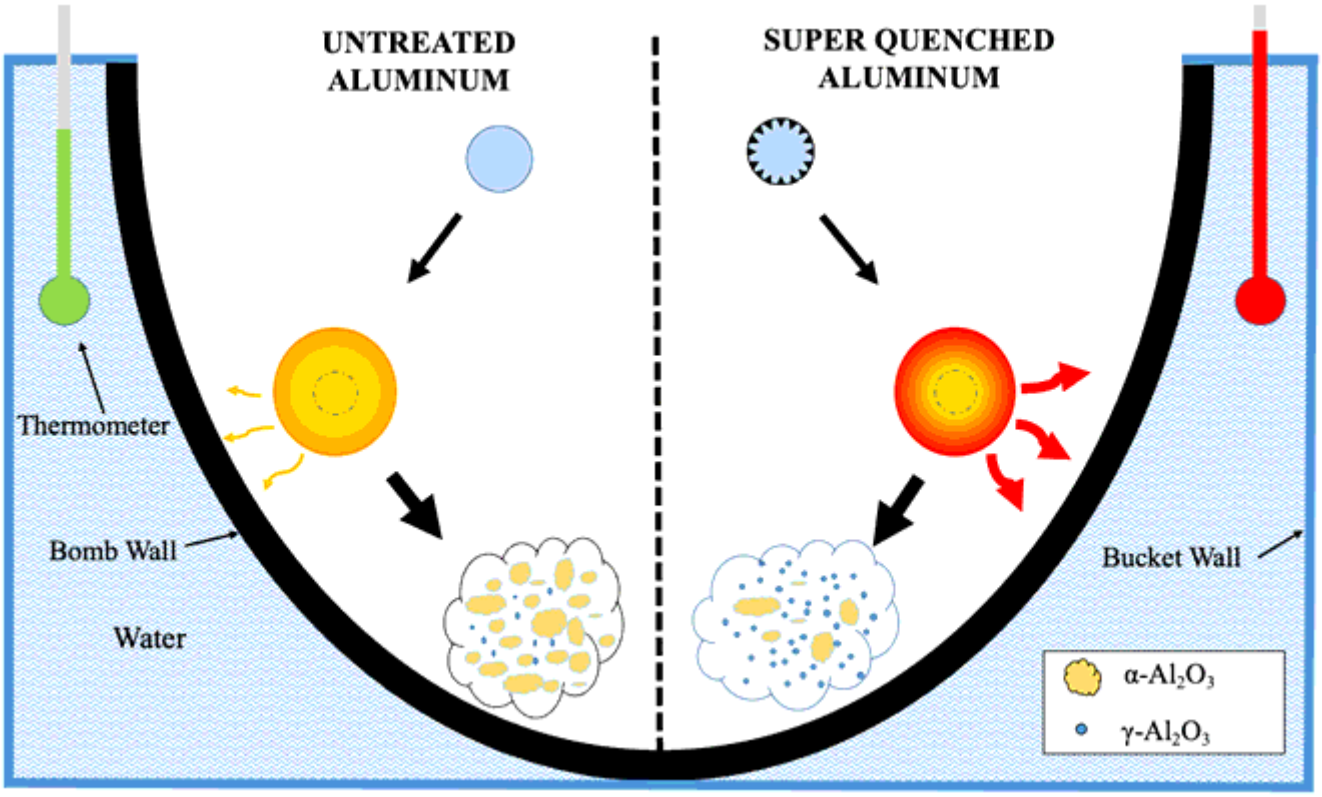

Figure 7

The schematic shown typical reaction inside the calorimeter bomb.

Supplementary Files

This is a list of supplementary files associated with this preprint. Click to download.

- SupplementaryInformationv5.docx